This article was downloaded by: [China Science & Technology University]
On: 27 November 2014, At: 01:27
Publisher: Taylor & Francis
Informa Ltd Registered in England and Wales Registered Number: 1072954 Registered office: Mortimer House, 37-41 Mortimer Street, London W1T 3JH, UK

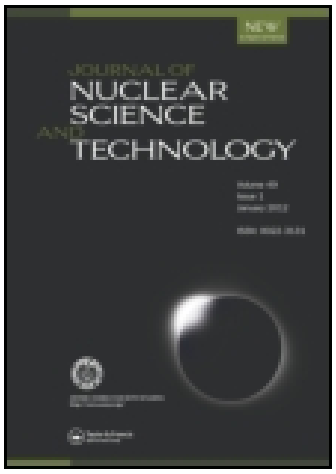

Journal of Nuclear Science and Technology
Publication details, including instructions for authors and subscription information:
http://www.tandfonline.com/loi/tnst20

Measurement of Alpha-Particles Emitted from Interaction of 14.6 MeV Neutrons with Elemental Nickel

Bangjiao YE [a] , Rongdian HAN [a] , Zhongmin WANG [a] , Yangmei FAN [a] , Xiaoqi YU [a] , Huaijiang DU [a] & Zhenxi XIAO [b]

[a] Department of Modern Physics , University of Science and Technology of China , Hefei , Anhui , 230027 , P.R. CHINA

[b] Institute of Management, University of Science and Technology of China , Beijing , 100088 , P.R. CHINA

Published online: 15 Mar 2012.

To cite this article: Bangjiao YE , Rongdian HAN , Zhongmin WANG , Yangmei FAN , Xiaoqi YU , Huaijiang DU & Zhenxi XIAO (1998) Measurement of Alpha-Particles Emitted from Interaction of 14.6 MeV Neutrons with Elemental Nickel, Journal of Nuclear Science and Technology, 35:1, 1-5, DOI: 10.1080/18811248.1998.9733813

To link to this article: http://dx.doi.org/10.1080/18811248.1998.9733813

PLEASE SCROLL DOWN FOR ARTICLE

Taylor & Francis makes every effort to ensure the accuracy of all the information (the "Content") contained in the publications on our platform. However, Taylor & Francis, our agents, and our licensors make no representations or warranties whatsoever as to the accuracy, completeness, or suitability for any purpose of the Content. Any opinions and views expressed in this publication are the opinions and views of the authors, and are not the views of or endorsed by Taylor & Francis. The accuracy of the Content should not be relied upon and should be independently verified with primary sources of information. Taylor and Francis shall not be liable for any losses, actions, claims, proceedings, demands, costs, expenses, damages, and other liabilities whatsoever or howsoever caused arising directly or indirectly in connection with, in relation to or arising out of the use of the Content.

This article may be used for research, teaching, and private study purposes. Any substantial or systematic reproduction, redistribution, reselling, loan, sub-licensing, systematic supply, or distribution in any form to anyone is expressly forbidden. Terms & Conditions of access and use can be found at http://www.tandfonline.com/page/terms-and-conditions

Journal of NUCLEAR SCIENCE and TECHNOLOGY, Vol. 35, No. 1, p. 1–5 (January 1998)

Measurement of Alpha-Particles Emitted from Interaction of 14.6 MeV Neutrons with Elemental Nickel

Bangjiao YE*,†, Rongdian HAN*, Zhongmin WANG*, Yangmei FAN*,
Xiaoqi YU*, Huaijiang DU* and Zhenxi XIAO**

* *Department of Modern Physics, University of Science and Technology of China*
** *Institute of Management, University of Science and Technology of China*

(Received February 3, 1997)

The double-differential cross sections (DDX) of α-particle emission from the reaction of 14.6 MeV neutrons with elemental nickel have been measured using a multitelescope system. The cross sections at sixteen reaction angles from 25° to 164.5° have been obtained. The angle-integrated spectrum and the angular distribution of α-particle emission have been deduced from the DDX. The total α-particle emission cross section was 102 ± 8 mb. The present result was compared with the evaluation of ENDF/B-VI and other measurements.

KEYWORDS: MEV range 10–100, neutrons, neutron reactions, double-differential cross sections, natural nickel, multitelescope system, nickel, alpha particles, angular distribution

Downloaded by [China Science & Technology University] at 01:27 27 November 2014

I. Introduction

Cross section data for the reactions of neutrons with structural materials to produce α-particles are very important for the evaluation of radiation damage and nuclear heating in fission and fusion reactors. The $(n, x\alpha)$ reaction leads to a buildup of helium gas, residual radioactivities, and the production of recoils from the lattice. It also induces nuclear transmutation, which can affect the structural strength of the materials. Theoretical understanding of the reaction is limited by the significant uncertainties in such quantities as the level density parameters, the pre-equilibrium process modeling, and the α-cluster preformation probabilities. At neutron energies around 14 MeV, several reaction channels open. Consequently, the $(n, x\alpha)$ reaction cross section is the sum of (n, α), $(n, n\alpha)$, $(n, \alpha n)$, and possibly $(n, 2\alpha)$ reaction cross sections.

Two methods are used to measure the helium production data. One method is the helium-accumulation method[1][2] with which only the helium-production cross section can be given. Another method is the direct detection of α-particles to obtain the double differential α-particle production cross section. With the latter one can obtain the angular distributions as well as the α-production cross sections. However, there are two problems in DDX measurements of low counting rates and high backgrounds. The latter are due to γ-rays coming from the $(n, n'\gamma)$, $(n, 2n)$ and (n, γ) reactions and the backgrounds are higher than the $(n, x\alpha)$ reaction counts by a factor of 10^3 to 10^6 for an unshielded detector.

Over the past 20 years, some new detection systems have been developed to detect α-particles, for example, the charged particle time-of-flight (TOF) spectrometer at Ohio University[3], the magnetic quadrupole spectrometer at Lawrence Livermore National Laboratory[4], the multitelescope systems at Vienna University[5] and University of Science and Technology of China (USTC)[6], and the wide range charged particle spectrometers at Tohoku University[7] and Los Alamos National Laboratory[8]. The energy spectra and angular distributions of emitted α-particles have been studied for some structural materials with these detection systems.

Since 1986 the researchers of USTC have built a multitelescope system similar to that of Vienna University[5]. The energy loss (ΔE) signal, the pulse-shape discrimination (PSD) signal and the energy (E) signal are gathered and their combinations are used to identify protons, α-particles and γ-rays. A thick target technique[9] has been employed to increase the event rates and decrease statistical errors. In this way it became possible to measure the high energy parts of the spectra with much better accuracy than with a thin target method, and also the results are much less sensitive to the backgrounds. Some (n, xp) reactions have been studied by using this system[10]-[12] This paper reports a measurement of DDX of α-particle emission from the ^{nat}Ni$(n, x\alpha)$ reaction at a neutron energy of 14.6 MeV using the USTC system.

II. Experimental System and Procedure

The USTC multitelescope system consists of a two-layer ring-shaped energy loss detector and a central CsI(Tl) energy detector as shown in **Fig. 1**. The outer layer of the energy loss detector consists of 32 separate proportional counter, which are used to obtain the energy loss signals (ΔE_1) of charged particles. The inner layer consists of 16 separate proportional counters, and their signals (ΔE_2) serve as one of the triple-coincidence

* *Hefei, Anhui 230027, P.R.CHINA.*
** *Beijing 100088, P.R.CHINA.*
† Corresponding author, Tel. +86-551-3601163(0), Fax. +86-551-3601164, E-mail: bjye@lx04.mphy.ustc.edu.cn

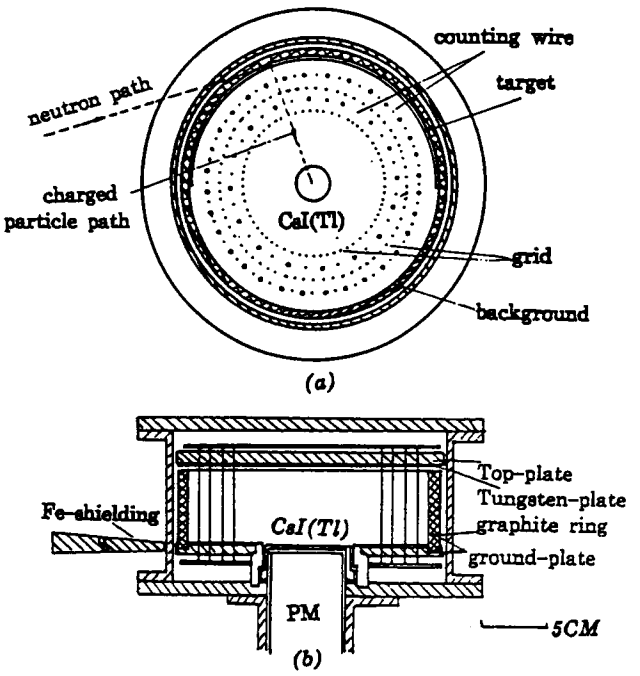

Fig. 1 The USTC multitelescope system: (a) top view and (b) side view

signals. A target foil was laid on one-half of the target holder (covered with a 0.3 mm lead foil) and a lead foil for background-measurement was placed on the other half of the target holder. Lead has very small cross sections of the (n, α) reaction (<1 mb). The two sets of outer 16 counters for both foils were used for simultaneous measurement of the foreground and background, respectively. The top- and ground-plates of detector system were covered with a 1-mm thick tungsten foil to stop all charged particles produced in the plates.

A CsI(Tl) crystal, 1 mm in height and 25.4 mm in diameter, was used as an energy detector. A 20-cm long Fe bar was used to shield the CsI(Tl) detector from neutrons. The distance between the neutron source (T–Ti target) and the CsI(Tl) was 400 mm. The angular acceptance function of each outer counter was calculated by using a Monte-Carlo method (10^6 events) according to geometric relation[13].

Each of the outer proportional counters, in conjunction with the central CsI(Tl) crystal, acts as a normal counter telescope that allows measurement of particle energy and identification of particles. The telescopes correspond to reaction angles of 25°, 32.8°, 43.9°, 55.0°, 67.2°, 77.1°, 88.3°, 98.3°, 108.6°, 117.9°, 128.0°, 136.6°, 144.3°, 151.9°, 157.8° and 164.5°.

The proportional counters were operated with a gas mixture of 95%Ar+5%CO_2 at a gas pressure of 0.01 MPa and at a voltage of −620 V.

An elemental nickel target with a 0.5 mm thickness and a 40 × 288 mm^2 area was used. The target thickness is selected to be thick enough to stop the maximum energy α-particles from the reaction.

Figure 2 is a simplified electronics block diagram. The electronics system consists of two parts: the electronic signal readout circuits and the CAMAC data collection system. For each $(n, x\alpha)$ reaction event, five signals, ΔE, E, PSD, TIME and ADDR, are recorded sequentially on a disk in an on-line computer.

A charged particle produced by a neutron-induced reaction at the target foil must traverse one of the outer proportional counters and produces both analog and digital (ADDRess readout) signals. The digital signal is fed to an address logic and transformed into five-bit address that identifies the active counting wire. The analog pulse is amplified, and fed into a linear gate. At last, all 32 analog signals are combined into one and fed into ADC.

The CsI(Tl) scintillator is used to produce both E and PSD signals. The PSD signal is fed into a slow coincidence (SC) circuit and the SC circuit produces an SC signal that acts as a strobing signal to open all ADC gates. The TIME signal was made by the time difference between the signals from one of the outer layer counters and the CsI(Tl) detector.

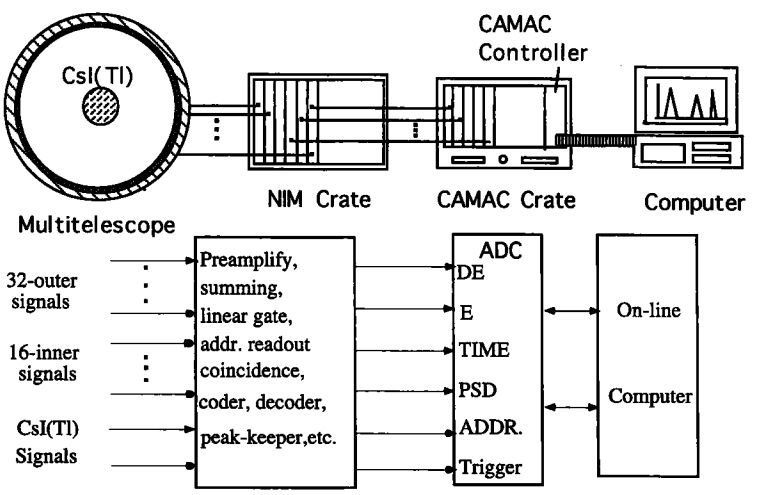

Fig. 2 Block diagram of the electronics system

Downloaded by [China Science & Technology University] at 01:27 27 November 2014

Downloaded by [China Science & Technology University] at 01:27 27 November 2014

A new intelligent CAMAC crate controller was designed to control the ADC circuits and communicate with the on-line computer. Data are recorded in a buffer region of the CAMAC crate controller. When the buffer region is full or the collection of data is completed, the data are read out and stored in a disk by the host computer.

Neutrons of 14.6 MeV were produced by a 150-kV Cockcroft-Walton accelerator at USTC. The target was irradiated for about 120 h at a neutron source strength of 3×10^9 n/s. The neutron flux was determined by using the associated α-particle method. During the entire experiment, one background telescope was equipped with a weak ^{241}Am α-source to monitor the energy calibration of the CsI(Tl) crystal. The energy resolution of the telescope is 8.0% for the 5.486 MeV α-particles from the ^{241}Am α-source. The stability of the entire measuring system was checked continually by monitoring count rates of the important signals. The target foil was rotated by 180° at the midpoint of the experiment to reduce asymmetry effects between the two different halves of the reaction chamber.

III. Data Analysis and Results

Data analysis was performed according to the following processes. First the PSD spectra and the ΔE spectra were used to discriminate particles. The PSD spectra show a good separation among protons, α-particles and γ-rays, as shown in **Fig. 3**. The two-dimensional spectra for combinations of two of ΔE, PSD and E signals were used for further discrimination of particles. **Figures** 4(a) to (c) show three two-dimensional spectra for ΔE-E, E-PSD and ΔE-PSD, respectively. From the ΔE-E spectrum we see that ΔE achieves good separation in the low energy region, while PSD shows good identification in the high energy region as shown in the E-PSD spectrum. Combining the two advantages we can identify particles clearly as seen in the ΔE-PSD spectrum. Then the chance coincidence counts were eliminated by using the TIME spectrum as shown in **Fig. 5**. Background counts were rejected by subtracting the background spectrum from the foreground spectrum channel by channel as shown in **Fig. 6**. After these processes the thick target α-particle emission spectra $N(\varepsilon, \theta)$ were obtained for the 16 reaction angles.

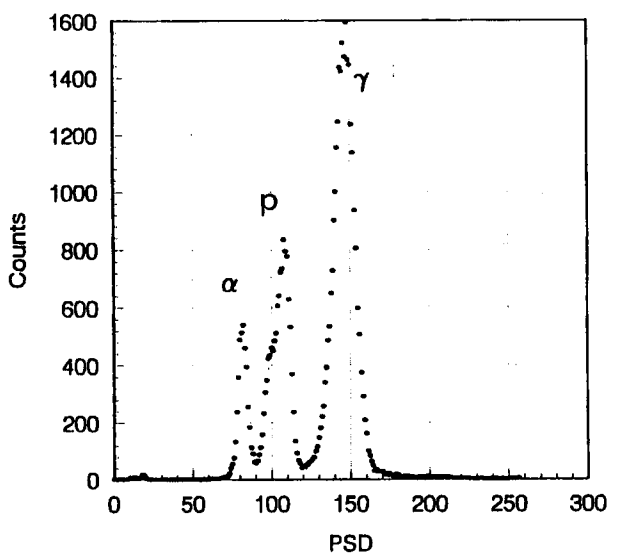

Fig. 3 PSD spectrum for the ^{nat}Ni(n, $x\alpha$) reaction

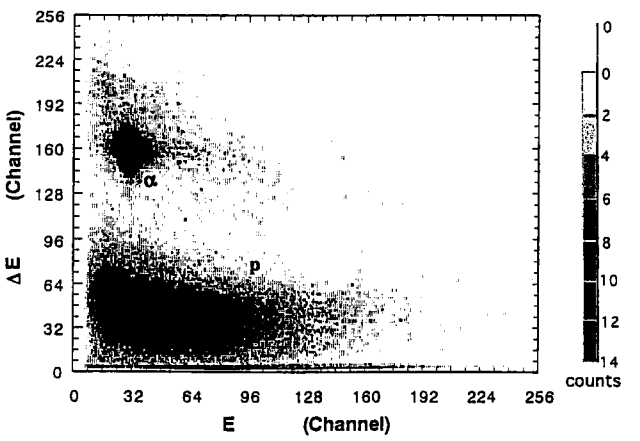

(a) ΔE-E spectrum

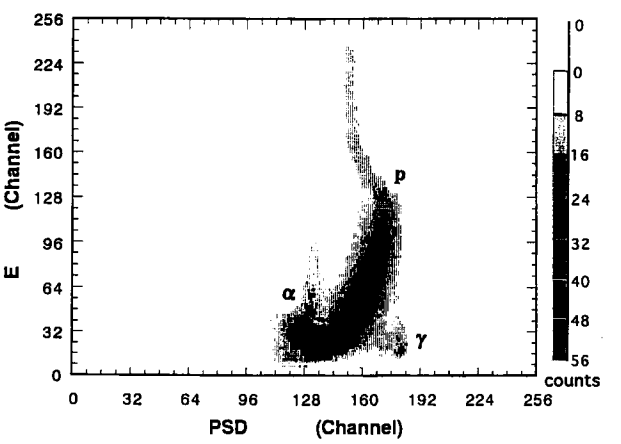

(b) E-PSD spectrum

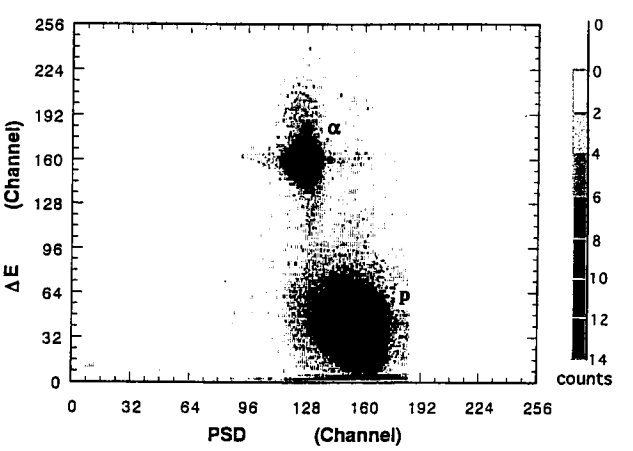

(c) ΔE-PSD spectrum

Fig. 4 Two-dimensional ΔE-E, E-PSD and ΔE-PSP spectrums

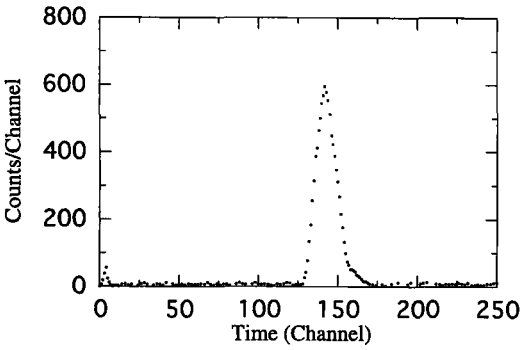

Fig. 5 Time spectrum of the ^{nat}Ni(n, $x\alpha$) reaction

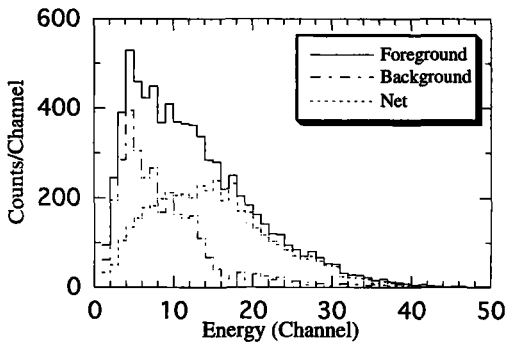

Fig. 6 Foreground, background and net energy spectra for the ^{nat}Ni(n, $x\alpha$) reaction at 25°

In order to obtain the double-differential α-particle emission cross sections, $N(\varepsilon, \theta)$ must be unfolded. This was done by numerically differentiating the quantity $N(\varepsilon, \theta)(d\varepsilon/dx)$ with respect to ε[9], where $(d\varepsilon/dx)$ is the specific energy loss for α-particles of energy ε[14].

First the energy spectrum $N(\varepsilon, \theta)$ was multiplied by the $(d\varepsilon/dx)(\varepsilon_i)$, where ε_i is the energy of channel i, and the resulting spectrum

$$\overline{N}(\varepsilon_i, \theta) = N(\varepsilon_i, \theta)\frac{d\varepsilon}{dx}(\varepsilon_i) \tag{1}$$

was differentiated by calculating

$$\frac{d}{d\varepsilon}\overline{N}(\varepsilon_i, \theta) = \overline{N}'(\varepsilon_i, \theta) = \frac{\overline{N}(\varepsilon_{i+1}, \theta) - \overline{N}(\varepsilon_{i-1}, \theta)}{\varepsilon_{i+1} - \varepsilon_{i-1}}, \tag{2}$$

giving the equivalent thin target spectrum. At last, the double-differential α-particle emission cross sections were obtained for the 16 reaction angles as the following:

$$\frac{d^2\sigma}{d\varepsilon d\Omega} = \frac{\Delta\overline{N}'(\varepsilon, \theta)}{\Delta\varepsilon\Delta\Omega\Phi_n S n\eta}, \tag{3}$$

where $\Delta\overline{N}'(\varepsilon, \theta)$ is the counts in the energy region of ε to $\varepsilon + \Delta\varepsilon$ and at the reaction angle θ, $\Delta\Omega$ the solid angle of the CsI(Tl) detector to the target, Φ_n the total neutron fluence, S the target area for each telescope, n the number of atoms in a unit volume and η is the detection efficiency. **Figure 7** shows the double-differential cross sections at the reaction angle 88.3°.

The data errors consist of statistical errors of 1σ and systematic errors. The total systematic error is 6.2%, which consists of the errors of the neutron flux 3.3%, the target height 2%, the solid angle of the central detector 3%, the $d\varepsilon/dx$ value 2%, and the data reduction procedure 2%, and other possible uncertainties 3%.

The angular distributions can be described well by a series of the Legendre polynomials up to $l = 2$

$$\frac{d^2\sigma}{d\varepsilon d\Omega} = \sum_{l=0}^{2} a_l P_l(\cos\theta). \tag{4}$$

The angle-integrated α-particle emission cross sections were derived from the least-squares fit of the Legendre polynomials up to $l = 2$ to the experimental $d^2\sigma/d\varepsilon d\Omega$ values. **Figure 8** shows the angle-integrated cross sections in comparison with the experimental results by Grimes *et al.*[4] and Baba *et al.*[7], and the ENDF/B-

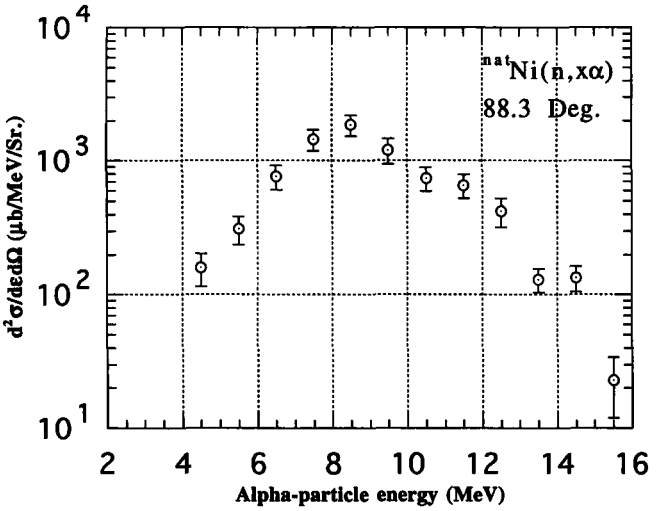

Fig. 7 Double-differential cross section of the ^{nat}Ni(n, $x\alpha$) reaction at 88.3° and at a neutron energy of 14.6 MeV

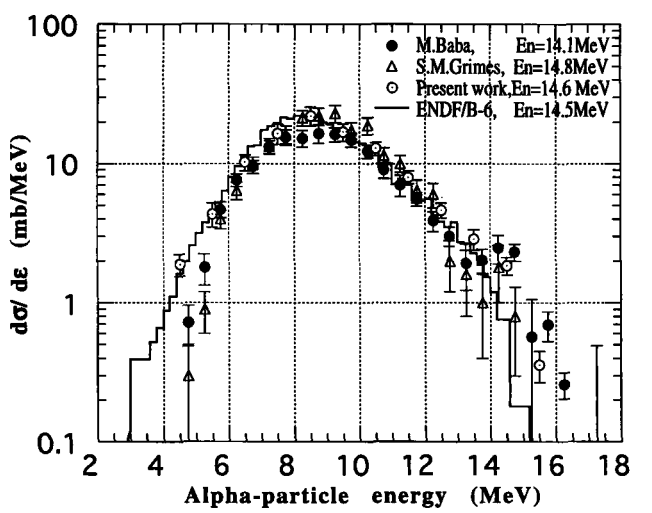

Fig. 8 Angle-integrated α-particle cross sections of the ^{nat}Ni(n, $x\alpha$) reaction

Downloaded by [China Science & Technology University] at 01:27 27 November 2014

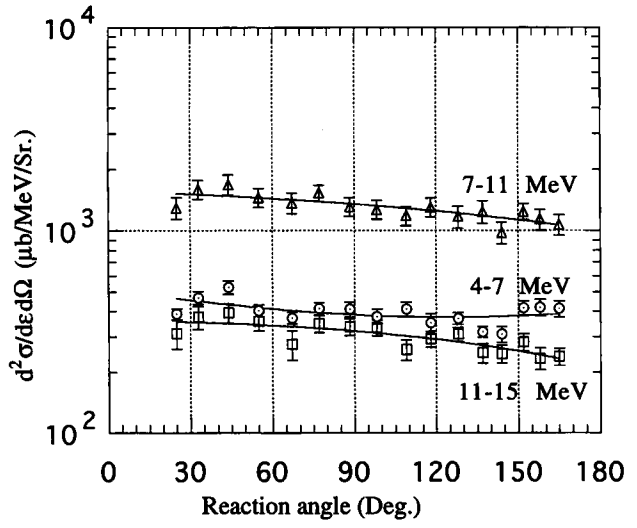

Fig. 9 Angular distribution of α-particle emission from the ^{nat}Ni(n, $x\alpha$) reaction

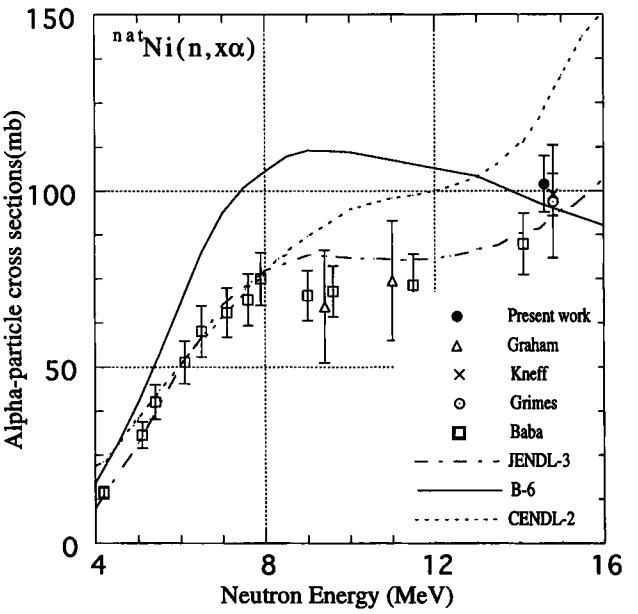

Fig. 10 Total ^{nat}Ni(n, $x\alpha$) reaction cross sections

VI evaluation. In the low energy region the present results are slightly higher than those of Grimes and Baba, but agree with their values within the quoted errors in the high energy region. The ENDF/B-VI evaluation is in good agreement with the present result in the low-energy region but slightly lower in the high-energy region.

The experimental angular distributions of the α-particles are shown in **Fig. 9**. In order to show the change of the angular distribution with the α-particle energy, angular distributions are shown for three α-particle energy regions of 4–7 MeV, 7–11 MeV and 11–15 MeV. They show a slight forward-backward asymmetry in the higher energy region and the equilibrium emission is dominant.

The total α-particle emission cross section is obtained as 102 ± 8 mb. **Figure 10** shows the total α-particle emission cross section of ^{nat}Ni in comparison with the experimental results by Graham *et al.*[15], Kneff *et al.*[16], Grimes *et al.*[4] and Baba *et al.*[7], and the evaluations by ENDF/B-VI[17], JENDL-3[18] and CENDL-2[19]. The present result is in agreement with the results of Grimes *et al.* and Kneff *et al.* within the range of error.

IV. Summary

We have measured the double-differential ^{nat}Ni(n, $x\alpha$) reaction cross section at a neutron energy of 14.6 MeV for 16 reaction angles using a multitelescope system. Particles have been identified by using two-dimensional ΔE-E E-PSD and ΔE-PSD spectra. A thick target technique was used to increase event rates and decrease statistical errors. The result is in good agreement with other experimental results.

ACKNOWLEDGMENT

The authors would like to express appreciation to Prof. M. Baba for providing his experimental data which have been used in this paper. We also acknowledge Dr. S. Chiba for his critical review of this paper. This work was supported in part by the General Company of Nuclear Industry of China and the Young Funds of USTC.

We thank the Atomic Energy Society of Japan for the generous support given in publishing this paper.

—REFERENCES—

(1) Haight, R. C., *et al.*: *Proc. Int. Conf. on Nuclear Data for Science and Technology*, Gatlinburg, p. 275 (1994).
(2) Takao, Y., *et al.*: *JAERI-Conf* 96-008, 165 (1996).
(3) Saraf, S. K., *et al.*: *Nucl. Sci. Eng.*, **107**, 365 (1991).
(4) Grimes, S. M., *et al.*: *Phys. Rev. C*, **17**, 508 (1978).
(5) Traxler, G., *et al.*: *Nucl. Instrum. Methods*, **217**, 121 (1983).
(6) Ye, B. J., *et al.*: *Commun. Nucl. Data Prog.*, **10**, 19 (1993).
(7) Baba, M., *et al.*: *Proc. Int. Conf. on Nuclear Data for Science and Technology*, Gatlinburg, p. 941 (1994).
(8) Sterbenz, S. M., *et al.*: *ibid.*, p. 925.
(9) Fischer, R., *et al.*: *Phys. Rev.*, C **37**, 578 (1988).
(10) Ye, B. J., *et al.*: *Nucl. Sci. Eng.*, **117**, 67 (1994).
(11) Ye, B. J., *et al.*: *Nucl. Sci. Eng.*, **122**, 136 (1996).
(12) Ye, B. J., *et al.*: *Nucl. Phys. A*, **612**, 213 (1997).
(13) Lin, G., *et al.*: *J. China Univ. Sci. Technol.* **25**, 25 (1995).
(14) Ziegler, J. F.: "*Helium Stopping Powers and Ranges in All Elemental Matter*", Pergamon Press, New York, (1997).
(15) Graham, S. L., *et al.*: *Nucl. Sci. Eng.*, **95**, 60 (1987).
(16) Kneff, D. W., *et al.*: *Nucl. Sci. Eng.*, **92**, 491 (1986).
(17) Evaluated Nuclear Data File (ENDF/B-VI) Summary Documentation, *BNL-NCS*-17541, (1991).
(18) Shibata, K., *et al.*: Japanese Evaluated Nuclear Data Library, Version-3 (JENDL-3), *JAERI*-1319, (1990).
(19) Zhou, D., Zhang, J., Liu, T.: Chinese Evaluated Nuclear Data Library (CENDL-2), Final Rep. for IAEA Contract Nr. 5962/R1/RB.

Downloaded by [China Science & Technology University] at 01:27 27 November 2014